

Melting behavior of large disordered sodium clusters

A. Aguado^a, L.M. Molina, J.M. López, and J.A. Alonso

Departamento de Física Teórica, Universidad de Valladolid, Valladolid 47011, Spain

Received 5 February 2001 and Received in final form 21 May 2001

Abstract. The melting-like transition in disordered sodium clusters Na_{92} and Na_{142} is studied by performing density functional constant-energy molecular dynamics simulations. The orbital-free version of the density functional formalism is used. In Na_{142} the atoms are distributed in two distinct shells (surface and inner shells) and this cluster melts in two steps: the first one, at ≈ 130 K, is characterized by the development of a high intrashell atomic mobility, and the second, homogeneous melting at ≈ 270 K, involves diffusive motion of all the atoms across the whole cluster volume. On the contrary, the melting of Na_{92} proceeds smoothly over a very broad temperature interval, without any abrupt change in the thermal or structural indicators. The occurrence of two steps in the melting transition is suggested to be related to the existence of a grouping of the atoms in radial shells, even if those shells present a large degree of internal disorder. It then appears that a cluster can be considered fully amorphous (totally disordered) only when there are no radial regions of low atomic density separating shells. The isomer of Na_{92} studied here fulfills this criterion and its thermal behavior can be considered as representative of that expected for fully amorphous clusters. Disordered Na_{142} , on the other hand, that has a discernible structure of an inner and a surface shell, should be considered as not fully disordered. The thermal behavior of these two clusters is also compared to that of icosahedral (totally ordered) sodium clusters of the same sizes.

PACS. 36.40.Ei Phase transitions in clusters – 64.70.Dv Solid-liquid transitions

1 Introduction

Cluster melting is a topic of current theoretical [1–8] and experimental [9–12] interest, motivated by the observation of several features which have no analog in the bulk phase. The most striking new feature is that the melting transition does not occur at a well defined temperature as in the solid, but spreads over a finite temperature interval that broadens as the cluster size decreases. The lower end of that interval defines the freezing temperature T_f below which the cluster is completely solidlike, their constituent atoms just vibrating about their equilibrium positions. The upper part of the interval defines the melting temperature above which all the atoms can diffuse across the cluster and the “liquid” phase is completely established. Between those two temperatures the cluster is not fully solid nor fully liquid [13]. It is in that transition region where the cluster-specific behavior emerges: (i) premelting effects, like partial melting of the cluster (the most usual case is surface melting) [14], or structural isomerizations upon heating [15], which lead to a melting in steps. (ii) The dynamical coexistence regime, where the cluster can fluctuate in time between being completely solid or liquid [16]. Also, strong nonmonotonic variations of the

melting temperature with size have been found in recent experiments on sodium clusters [10]. Both electronic and atomic shell effects can be responsible for this interesting behavior. The values of T_f and T_m as defined above are not yet amenable to the experiments, and the experimental melting temperature is somewhere between those two values.

Previously we have reported orbital-free density functional molecular dynamics (OFMD) simulations of the melting process for icosahedral alkali clusters [6–8]. The OFMD technique [17] is analogous to the Car-Parrinello (CP) method to perform dynamical simulations at an *ab initio* level [18], but the electron density is taken as the dynamical variable [19] in the OFMD, as opposed to the Kohn-Sham (KS) orbitals [20] in the original CP method. This technique has been used before both in solid state [21, 22] and cluster [2, 23, 24] physics. Its main advantage over KS-based methods is that the computational effort to update the electronic system increases linearly with the cluster size N , in contrast to the N^3 scaling of methods based on orbitals. Indeed, our previous calculations [7, 8] were the first molecular dynamics simulations of such large clusters as A_{92} and A_{142} , with $\text{A} = \text{Na}, \text{K}, \text{Rb}, \text{Cs}$, that included an explicit treatment of the electronic degrees of freedom. This “explicit treatment of the electronic degrees of freedom” is, however, only approximate as quantum-shell effects are not reproduced by the specific electronic kinetic energy functional employed in this work (see next section). Thus, whatever the effect

^a *Present address:* Physical and Theoretical Chemistry Laboratory, University of Oxford, South Parks Road, Oxford OX1 3QZ, UK.

e-mail: aguado@joule.pcl.ox.ac.uk

on cluster melting associated with electronic shell closings may be, it will not be properly described by our calculations, which thus should be considered as quite useful in finding generic effects but not as fully predictive at a quantitative level.

An important issue in the simulations of cluster melting is the the low-temperature isomer to be heated, as the details of the melting transition are known to be isomer-dependent [25]. The problem of performing a realistic global optimization search of the structure of a cluster becomes exponentially difficult as its size increases, so finding the low temperature global minimum of Na_{92} and Na_{142} becomes a hard task. Our numerous geometry optimizations by an unconstrained search method such as simulated annealing, starting with randomly generated structures, always have led to disordered isomers both for Na_{92} and Na_{142} . On the other hand, in previous work [7, 8] we have studied the melting of icosahedral isomers, as there are some experimental [9] and theoretical [26] indications that suggest icosahedral packing in large alkali clusters. Those icosahedral structures are, in fact, energetically more stable than the disordered ones for Na_{92} and Na_{142} at the OF level, and we obtained good agreement for the melting temperatures with the experimental results of Haberland's group [10]. Although the disordered structures are less stable at the OF level, the energy difference between icosahedral and disordered isomers is only about 0.02 eV/atom, which is very small. Amorphous-like structures have been found recently to be the ground state of gold clusters for a number of sizes [27, 28], and pair potential calculations performed by Doye and Wales predict that amorphous structures are favored by long potential ranges [29]. The specific features of those structures are little or no spatial symmetry and a pair distribution function typical of glasses. Besides, one usually finds a large number of amorphous isomers nearly degenerate in energy, which suggests that they occupy a substantial fraction of the phase space available to the cluster. Both the proximity in energy to the more stable icosahedral isomers and the large entropy associated with the amorphous part of the phase space make plausible that disordered isomers could be present in the cluster beams, so their thermal properties deserve specific investigation. Apart from this, the study of melting in amorphous-like clusters is intriguing from a theoretical point of view. Thus the goals of this work are to study the mechanisms by which the melting-like transition proceeds in the disordered isomers of Na_{92} and Na_{142} , to study the influence of the degree of disorder on the melting behavior, and to make a meaningful comparison with the melting of the icosahedral isomers. In the next section we briefly present some technical details of the method. The results are presented and discussed in Section 3 and, finally, Section 4 summarizes our main conclusions.

2 Theory

The details of our implementation of the orbital-free Car-Parrinello scheme have been described in previous

work [6–8], so we just present briefly the main technical issues. The electronic kinetic energy functional of the electron density is approximated by the gradient expansion around the homogeneous limit through second order [19, 30–32]. This means that we keep the local Thomas-Fermi term and the lowest order density gradient correction. The local density approximation is used for exchange and correlation [33, 34]. The ionic field acting on the electrons is represented by the local pseudopotential of Fiolhais *et al.* [35]. The cluster is placed in a unit cell of a cubic superlattice with edge 71 a.u. and the set of plane waves periodic in that superlattice, up to an energy cutoff of 8 Ry, is used as a basis set to expand the valence density. Following Car and Parrinello [18], the coefficients of that expansion are regarded as generalized coordinates of a set of fictitious classical particles, and the corresponding Lagrange equations of motion for the ions and the electron density distribution are solved as described in references [6, 7]. A $64 \times 64 \times 64$ grid was used, and the fictitious mass associated with the electron density coefficients ranged between 1.0×10^8 and 3.3×10^8 a.u. The equations of motion were integrated using the Verlet algorithm [36] for both electrons and ions, with a time step ranging from $\Delta t = 0.73 \times 10^{-15}$ s for the simulations performed at the lowest temperatures to $\Delta t = 0.34 \times 10^{-15}$ s for those at the highest temperatures. These choices resulted in a conservation of the total energy better than 0.1%. Several molecular dynamics simulation runs at different constant energies were performed in order to obtain the caloric curve for each cluster. The initial positions of the atoms for the first run were taken by slightly deforming the starting low temperature geometry of the cluster. The final configuration of each run served as the starting geometry for the next run at a different energy. The initial velocities for every new run were obtained by scaling the final velocities of the preceding run. The total simulation time was 20 ps for each run at constant energy.

The theoretical indicators employed to locate the melting-like transition were: (a) the caloric and specific heat curves as a function of the internal cluster temperature, which is defined through the equipartition theorem for the ionic kinetic energy; (b) the diffusion coefficient, obtained from the long time behavior of the mean square displacement; (c) the time evolution of the distances between each atom and the center of mass of the cluster; and (d) the microcanonical average of the atomic distribution function, defined by

$$dN_{\text{at}}(r) = g(r)dr, \quad (1)$$

where $dN_{\text{at}}(r)$ is the number of atoms at distances from the center of mass between r and $r + dr$. These indicators are the same as those used in previous publications [6–8].

3 Results

Our purpose is to analyze the melting of disordered clusters, so we now indicate how those clusters have been prepared. For this purpose dynamical annealing runs [18]

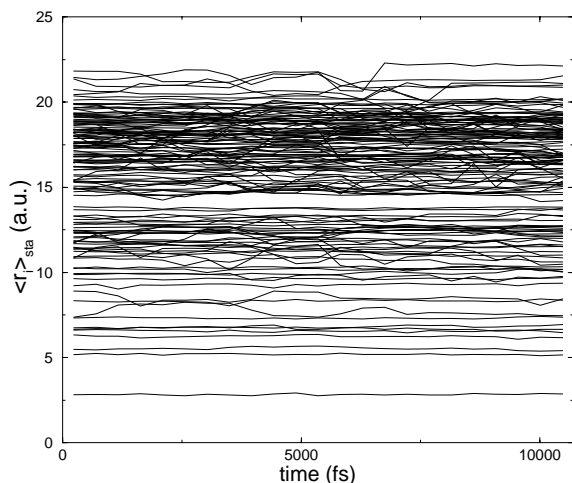


Fig. 1. Short-time averaged distances $\langle r_i(t) \rangle_{sta}$ between each atom and the center of mass in a disordered isomer of Na_{142} at $T = 47$ K, as functions of time.

were started from high-temperature liquid isomers thermalized during 30 ps at 600 K. This thermalization was achieved by re-scaling the ion velocities after each molecular dynamics time-step in order to maintain the desired temperature. Once the clusters had been thermalized at 600 K, the cooling strategy was to reduce the internal cluster temperature along a OFMD annealing run. This reduction in temperature was achieved by multiplying the values of the ion velocities by 0.9999 after every twelve time steps. With the chosen time step of 0.34×10^{-15} s the temperature reduction is applied approximately every four femtoseconds. A first important difference between the low temperature icosahedral and disordered isomers is that the former ones have a faceted and smoother surface. Besides that, no apparent spatial symmetry is observed in the disordered isomers. In Figure 1 we show the short-time averages (sta) of the distances between each atom and the center of mass of the cluster for the disordered isomer of Na_{142} , obtained from an OFMD run at a low temperature ($T = 47$ K). The values of $\langle r_i(t) \rangle_{sta}$ are almost independent of time, indicating that the cluster is solid. A similar analysis for an icosahedral isomer of Na_{142} shows a grouping of the atoms in characteristic concentric atomic shells [7], while the lines in Figure 1 are quite dispersed. Nevertheless, there is a narrow interval at ≈ 14 a.u. where the ionic density is very low, that serves to define separate surface and inner regions. The case of Na_{92} , not shown here, is similar, although in that case the structure is even more uniformly amorphous, and there is no way to distinguish between surface and inner shells by this criterion. We will see below that this small difference between Na_{142} and Na_{92} is important. Soler *et al.* [27, 28] have compared the structures of icosahedral and amorphous gold clusters, with similar results: while the atoms in the icosahedral isomers are grouped in atomic shells, in the case of amorphous clusters there are “atomic transfers” between shells that blur the shell structure. For the gold clusters, the amorphous isomers turn out to be the

minimum energy structures for a number of sizes [27]. As mentioned above, in the case of Na_{92} and Na_{142} the icosahedral isomers are more stable at the OF level than the lowest energy disordered isomers found (by 0.017 eV/atom and 0.020 eV/atom for Na_{92} and Na_{142} respectively).

One of the predictions of this paper is the existence of a set of disordered structural isomers of Na clusters which are energetically very close to the icosahedral ones. Given the approximate nature of the OF methodology (with the employed electronic kinetic energy functional), additional DFT calculations at the KS level have been performed in order to check the quantitative accuracy of such a prediction.

We have used the *ab initio* fhi96MD code, developed by Scheffler *et al.* [37], based on the DFT and the LDA for exchange and correlation [33]. This code uses nonlocal pseudopotentials for the electron-ion interactions and a plane-wave expansion of the electronic wavefunctions, with a plane-wave cutoff of 8 rydbergs. The calculations were performed in a superlattice configuration, and hexagonal unit cells with lattice parameters $a = c = 50$ a.u., and $a = c = 52$ a.u. were used for Na_{92} and Na_{142} , respectively; those sizes make interactions between clusters in neighbouring cells negligible. Initial structures obtained from OF relaxed geometries were optimized until the corresponding *ab initio* local energy minimum was found. This optimization was performed using a damped Newtonian algorithm after several steps of the electronic structure minimization, iterated until the force on each atom was considered small enough (lower than 0.0001 hartree/a.u.).

For Na_{142} , the KS results predict the icosahedral isomer to be 0.02 eV/atom more stable than the disordered structure, in almost exact agreement with the OF predictions. For this size the main effect of the additional geometry optimization at the KS level was a global contraction of all interatomic distances by roughly 5%, with the isomers shape preserved to a good accuracy. In the case of Na_{92} , both isomers restructure more appreciably with respect to the OF predictions, and the final result is that the disordered isomer is more stable than the icosahedral one by only 0.001 eV/atom. As this energy difference is one order of magnitude smaller than that found for Na_{142} , these two isomers should be considered as essentially degenerate at the KS level. As a thorough search for the GS structure of Na_{92} has not been performed, the existence of ordered structures different from that considered here and lower in energy than the amorphous isomer has not been completely ruled out. The main message to be extracted from the KS calculations is that the OF prediction concerning the existence of energetically competitive disordered structures is supported. The radial ordering of the disordered structures is not qualitatively altered either by the KS calculations.

The specific heat of disordered Na_{142} (Fig. 2) displays two peaks, suggestive of a two-step melting process. The two peaks, at temperatures $T_s^{\text{dis}} \approx 130$ K and $T_m^{\text{dis}} \approx 270$ K respectively, are well separated, whereas these were found to lie much closer together for the corresponding icosahedral cluster of the same size, $T_s^{\text{ico}} \approx 240$ K

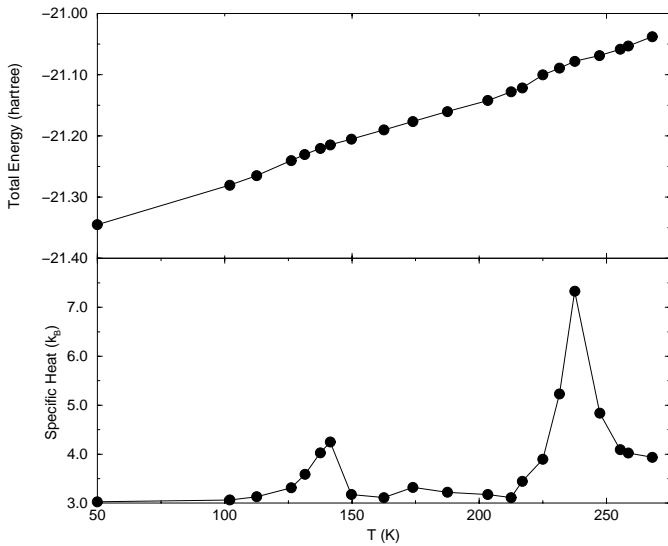


Fig. 2. Caloric and specific heat curves of a disordered isomer of Na_{142} , taking the internal cluster temperature as the independent variable. The deviation around the mean temperature is smaller than the size of the circles.

and $T_m^{\text{ico}} \approx 270$ K [7]. These results suggest that the melting transition starts at a temperature T_s and finishes at T_m with the difference in the melting between the two isomers being the smaller T_s value of the disordered isomer. In our previous work [7] we showed that for the icosahedral cluster those two steps can be identified with surface melting and homogeneous melting, respectively. A similar explanation is valid for the disordered Na_{142} isomer. At $T = 160$ K, a temperature between T_s^{dis} and T_m^{dis} , the structure of the disordered cluster is more fluid than at low temperature. Figure 3 indicates that the atomic shells have separately melted, and the atoms undergo diffusive motions mainly on a given shell, as seen in the bold lines, without an appreciable intershell diffusion. Although some occasional intershell displacements have been observed, these occur on a substantially longer time-scale as compared to intrashell displacements. The larger spread of the upper bold line indicates that diffusion is appreciably faster in the surface shell. Thus the transition at 130 K can be identified with intrashell melting. That is, the cluster melts, both its surface and internal parts, but the surface-shell atoms remain on the cluster surface without exchanging with the inner atoms. At this temperature the cluster behaves as formed by two immiscible – core and mantle – fluids. Why this occurs at a rather low temperature is associated with the large spread in the distribution of radial distances of the atoms in each shell. The atomic shells are structurally disordered at low temperature, although kinetically frozen, like in a typical glass, so inducing defects and diffusion in the shells of that cluster is rather easy and occurs at moderate temperatures. Surface melting does not develop in the icosahedral isomer until a temperature of $T_s^{\text{ico}} \approx 240$ K is reached. At this temperature, the time evolution of the distances of surface atoms to the cluster center for the icosahedral isomer [7]

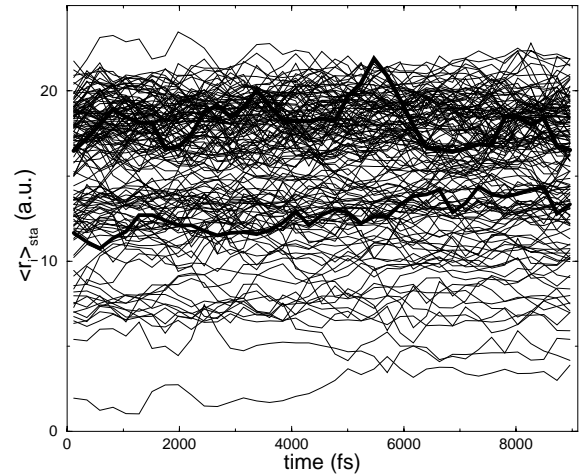


Fig. 3. Short-time averaged distances $\langle r_i(t) \rangle_{\text{sta}}$ between each atom and the center of mass in a disordered isomer of Na_{142} at $T = 160$ K, as functions of time. The bold lines follow the evolution of a particular atom in the surface shell and another in the inner part.

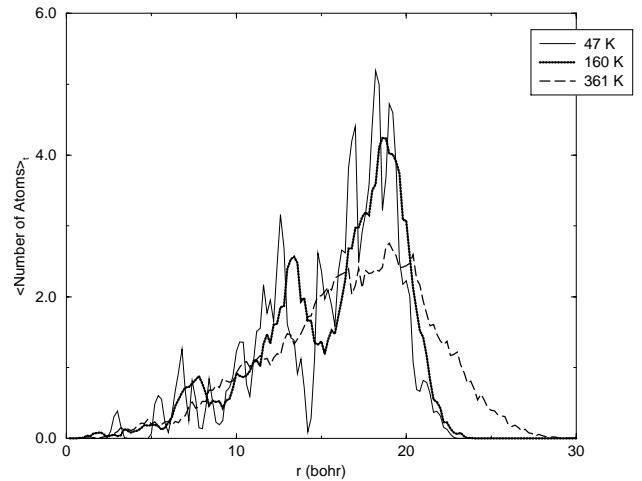


Fig. 4. Time averaged radial atomic density distribution in a disordered isomer of Na_{142} , at some representative temperatures.

becomes similar to that of the disordered Na_{142} isomer at 160 K. Inducing diffusion in the surface of the icosahedral isomer requires a higher temperature because of the higher structural order of the surface. Once the surface of both isomers has melted, homogeneous melting occurs at the same temperature, ≈ 270 K, in very good agreement with the experimental value of 280 K [10]. At that temperature the liquid phase is completely established (all atoms can diffuse across the whole cluster volume) and differentiating between the two isomers makes no sense anymore.

The thermal behavior of the two isomers discussed is thus not so different. The radial atomic density of the disordered isomer at 160 K, given in Figure 4, shows a smoothed shape compared to that at low T , but a distribution of the atoms in separate surface and inner atomic shells can still be distinguished. In our view, in spite of the high disorder in both surface and inner shells, the cluster

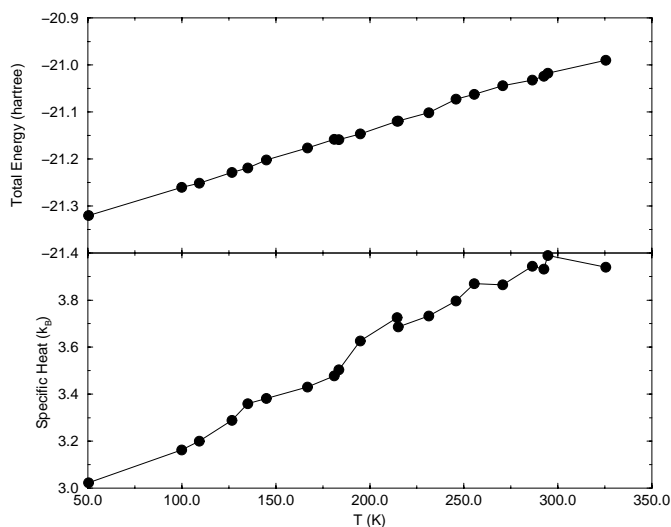


Fig. 5. Caloric and specific heat curves of disordered Na_{92} , taking the internal cluster temperature as the independent variable. The deviation around the mean temperature is smaller than the size of = the circles.

can not be considered as fully disordered. There are still some additional similarities. In reference [7], we showed that the solid-like phase of the icosahedral isomer ends at a temperature of 130 K, even though no peak is detected in the specific heat: isomerization transitions between different permutational isomers develop which preserve the icosahedral structure. Thus, both isomers depart from the solid-like phase at ≈ 130 K, the only difference being that one has direct access to the intrashell melting stage while the other enters first an isomerization regime. Calvo and Spiegelmann [5] have related the appearance of peaks in the specific heat to sudden openings of the available phase space. In the isomerization regime the icosahedral cluster has access just to a limited number of symmetry-equivalent isomers, while the phase space of the disordered cluster opens suddenly to include a very large number of isomers, as the shell has no prescribed structure. Thus, a peak in the specific heat appears at $T \approx 130$ K for the disordered isomer, but not for the icosahedral isomer. When homogeneous melting occurs, any sign of atomic shells in the time average of $g(r)$ disappears (Fig. 4).

The results for disordered Na_{92} are shown in Figure 5. This isomer melts gradually over a wide temperature interval, and neither appreciable specific heat peaks nor significant slope changes in the caloric curve are detected. This is in contrast to icosahedral Na_{92} , where a well defined two-step melting transition was detected [7]. In their simulations Ercolessi *et al.* [39] have also found a melting process without a latent heat of fusion for amorphous gold clusters with less than ~ 90 atoms. In Figure 6 we show the radial ionic density distribution of disordered Na_{92} at several temperatures. Even at a temperature as low as 70 K there is no discernible atomic shell structure (this feature should be compared to the case of Na_{142} given in Fig. 4). At an intermediate temperature, $T = 165$ K, the $g(r)$ function is similar to that for low temperature

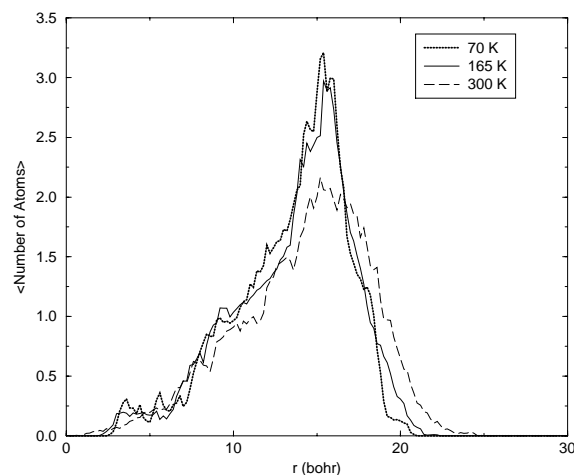


Fig. 6. Time averaged radial atomic density distribution of disordered Na_{92} , at some representative temperatures.

(we notice that at this intermediate temperature the surface of the corresponding icosahedral isomer has already melted [7]). At the higher temperature $T = 300$ K the only appreciable additional change of $g(r)$ in Figure 6 is due to the thermal expansion of the cluster. At this temperature the corresponding icosahedral isomer is liquid [7].

Comparing the structures of the disordered isomers of the two clusters Na_{142} and Na_{92} at low T , one concludes that Na_{92} is closer to a nearly ideal amorphous cluster since the radial atomic distribution function shows no sign of atomic shells. The disordered structure is kinetically frozen, but there seems to be no barriers preventing the full exploration of the liquid part of the phase space. In fact, Figure 6 shows that the cluster is already in that region of the phase space at low temperature. This can be seen more clearly in the evolution of the diffusion behavior with temperature. Figure 7 shows the temperature variation of the square root of the diffusion coefficient for the two Na_{92} isomers, the icosahedral and the disordered one. While the two steps in the melting of the icosahedral isomer become reflected as abrupt slope changes of \sqrt{D} , the value of \sqrt{D} for the disordered isomer increases with temperature in a smooth way, without any abrupt change. Thus, the opening of the available phase space proceeds in a gradual way and peaks in the specific heat are not detected. A similar plot for Na_{142} (not shown explicitly) reveals abrupt slope changes in both icosahedral and disordered isomers.

We have found a very different thermal behavior for two clusters that were both initially classified as disordered. Although it is not possible to draw general conclusions we think that these two examples are representative of two different classes of disordered clusters. The thermal behavior of Na_{92} represents that typical of a truly amorphous-like sodium cluster. In line with the discussion of “atomic transfers” between shells advanced by Soler *et al.* [28], we propose that a cluster can be considered completely amorphous only when no local regions with low atomic density exist in the radial atomic distribution

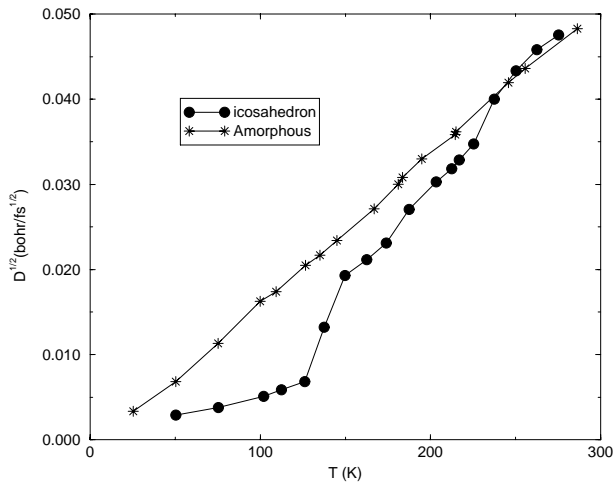


Fig. 7. Square root of the diffusion coefficient as a function of temperature for the icosahedral and amorphous isomers of Na_{92} .

around the cluster centre. The existence of distinct low atomic density regions, separating the cluster in broad shells as is the case for the disordered isomer of Na_{142} , is associated to another class of disordered clusters having some radial order. These radial correlations lead to substantial free energy barriers in the potential energy surface of the cluster, so sudden access to a substantial region of the available phase space is expected only above a certain temperature, and peaks appear in the temperature dependence of the specific heat. On the contrary, the absence of such radial correlations facilitates the diffusion of atoms across the whole cluster volume right from the start of the heating process. As the liquid-like phase becomes established when all the atoms of the cluster can diffuse across the cluster volume, we expect that no appreciable free energy barriers will be found in this case, and no peaks in the specific heat will be detected.

4 Summary and conclusions

The melting-like transition in disordered Na_{142} and Na_{92} has been investigated and compared to that of icosahedral isomers of the same sizes [7] by applying an orbital-free, density-functional molecular dynamics method. The computational effort which is required is modest in comparison with the Car-Parrinello Molecular Dynamics technique based on Kohn-Sham orbitals, that would be very costly for clusters of that size.

A disordered isomer of Na_{142} melts in two steps. The transition at $T_s^{\text{dis}} \approx 130$ K is best described as intrashell melting. This is followed by homogeneous melting at $T_m^{\text{dis}} \approx 270$ K. The details of the melting process depend on the starting low-temperature isomer, as those two stages lie much closer in temperature, 240 K and 270 K respectively [7], for the icosahedral Na_{142} isomer. In the disordered isomer there is not a distinct isomerization regime

(something rather evident because there is not an underlying ordered structure in each shell). Nevertheless the melting proceeds in steps because the atoms are grouped in two shells. Consequently, the melting of the two isomers of Na_{142} is not as different.

Icosahedral Na_{92} was found to melt also in two well defined steps in a previous publication [7]. The melting of a disordered isomer proceeds, instead, gradually, and spreads over a wide temperature interval. The thermal indicators as the calorific curve or the specific heat do not show any sign of an abrupt transition, which means that the phase space available to the cluster does not increase suddenly at any given temperature. The diffusion coefficient increases with temperature in a smooth way also, in contrast to the behavior shown by the corresponding icosahedral isomer. We suggest that the absence of an abrupt transition is closely related to the absence of shell structure in the radial atomic distribution; this absence of radial shell structure is viewed as a condition for a cluster to be considered completely amorphous. In this sense only the disordered isomer of Na_{92} that we have studied can be considered fully amorphous, while the disordered Na_{142} isomer shows radial correlations that turn it not fully amorphous.

From the results of this article and those found previously for the melting of icosahedral sodium clusters [7], we can draw some conclusions about the effect of structure on the melting properties of sodium clusters. A melting in steps is expected in *most* clusters showing a radial grouping of the atoms in shells, as is the case of the two studied isomers of Na_{142} (the icosahedral and the disordered one) and the icosahedral isomer of Na_{92} . In those cases, intrashell diffusive motion starts at a temperature T_{intra} , lower than the temperature T_{inter} at which intershell diffusive motion begins to be important. The separation between T_{intra} and T_{inter} is small if the internal order within the shells is high (for example, in the icosahedral cluster) and the number of defects in each shell is small: this occurs for icosahedral Na_{142} , with just five vacancies in the surface shell. A limiting case within the class of shell-clusters is represented by icosahedral Na_{55} . With two complete shells, and thus no defects, intrashell displacements are as difficult as intershell motions and the two temperatures T_{intra} and T_{inter} merge into a single one [7]. On the contrary when a shell contains a large number of defects the two temperatures are well separated: this is the case for icosahedral Na_{92} , with many vacancies in the surface shell, and also for the disordered Na_{142} isomer, in which the internal disorder within the individual shells is large. Finally, a gradual melting process with no abrupt transitions is expected for those disordered clusters with no sign of shells, that is for the fully amorphous-like clusters: this is the case of amorphous Na_{92} .

This work has been supported by DGES (Grants PB98-0345 and PB98-0368) and Junta de Castilla y León (Grants VA29/99 and VA70/99). The authors acknowledge the contribution of M.J. Stott to the development of the computer code that we used for this work.

References

1. A. Bulgac, D. Kusnezov, Phys. Rev. Lett. **68**, 1335 (1992); Phys. Rev. B **45**, 1988 (1992); N. Ju, A. Bulgac, Phys. Rev. B **48**, 2721 (1993); M. Fosmire, A. Bulgac, *ibid.* **52**, 17509 (1995); J.M. Thompson, A. Bulgac, *ibid.* **40**, 462 (1997); L.J. Lewis, P. Jensen, J.L. Barrat, *ibid.* **56**, 2248 (1997); S.K. Nayak, S.N. Khanna, B.K. Rao, P. Jena, J. Phys. Cond. Matt. **10**, 10853 (1998); F. Calvo, P. Labastie, J. Phys. Chem. B **102**, 2051 (1998); J.P.K. Doye, D.J. Wales, Phys. Rev. B **59**, 2292 (1999); J. Chem. Phys. **111**, 11070 (1999).
2. P. Blaise, S.A. Blundell, C. Guet, Phys. Rev. B **55**, 15856 (1997).
3. A. Rytkönen, H. Häkkinen, M. Manninen, Phys. Rev. Lett. **80**, 3940 (1998).
4. C.L. Cleveland, W.D. Luedtke, U. Landman, Phys. Rev. Lett. **81**, 2036 (1998); Phys. Rev. B **60**, 5065 (1999).
5. F. Calvo, F. Spiegelmann, Phys. Rev. Lett. **82**, 2270 (1999); J. Chem. Phys. **112**, 2888 (2000).
6. A. Aguado, J.M. López, J.A. Alonso, M.J. Stott, J. Chem. Phys. **111**, 6026 (1999).
7. A. Aguado, J.M. López, J.A. Alonso, M.J. Stott, J. Phys. Chem. B **105**, 2386 (2001).
8. A. Aguado, Phys. Rev. B **63**, 115404 (2001).
9. T.P. Martin, Phys. Rep. **273**, 199 (1996).
10. M. Schmidt, R. Kusche, W. Kronmüller, B. von Issendorff, H. Haberland, Phys. Rev. Lett. **79**, 99 (1997); M. Schmidt, R. Kusche, B. von Issendorff, H. Haberland, Nature **393**, 238 (1998); R. Kusche, Th. Hippler, M. Schmidt, B. von Issendorff, H. Haberland, Eur. Phys. J. D **9**, 1 (1999).
11. M. Schmidt, C. Ellert, W. Kronmüller, H. Haberland, Phys. Rev. B **59**, 10970 (1999).
12. H. Haberland, in *Metal Clusters*, edited by W. Ekardt (John Wiley & Sons, 1999), p. 181.
13. J. Jellinek, T.L. Beck, R.S. Berry, J. Chem. Phys. **84**, 2783 (1986).
14. Z.B. Güvenc, J. Jellinek, Z. Phys. D **26**, 304 (1993).
15. V.K.W. Cheng, J.P. Rose, R.S. Berry, Surf. Rev. Lett. **3**, 347 (1996).
16. H.P. Cheng, R.S. Berry, Phys. Rev. A **45**, 7969 (1991); R.S. Berry, in *Clusters of Atoms and Molecules*, edited by H. Haberland (Springer, Berlin, 1994), pp. 187–204.
17. M. Pearson, E. Smargiassi, P.A. Madden, J. Phys.: Cond. Matt. **5**, 3221 (1993).
18. R. Car, M. Parrinello, Phys. Rev. Lett. **55**, 2471 (1985); M.C. Payne, M.P. Teter, D.C. Allan, T.A. Arias, J.D. Joannopoulos, Rev. Mod. Phys. **64**, 1045 (1992).
19. P. Hohenberg, W. Kohn, Phys. Rev. **136**, 864B (1964).
20. W. Kohn, L.J. Sham, Phys. Rev. **140**, 1133A (1965).
21. E. Smargiassi, P.A. Madden, Phys. Rev. B **49**, 5220 (1994); M. Foley, E. Smargiassi, P.A. Madden, J. Phys.: Cond. Matt. **6**, 5231 (1994); E. Smargiassi, P.A. Madden, Phys. Rev. B **51**, 117 (1995); *ibid.* **51**, 129 (1995); M. Foley, P.A. Madden, *ibid.* **53**, 10589 (1996); B.J. Jesson, M. Foley, P.A. Madden, *ibid.* **55**, 4941 (1997); J.A. Anta, B.J. Jesson, P.A. Madden, *ibid.* **58**, 6124 (1998).
22. N. Govind, Y.A. Wang, E.A. Carter, J. Chem. Phys. **110**, 7677 (1999).
23. V. Shah, D. Nehete, D.G. Kanhere, J. Phys.: Cond. Matt. **6**, 10773 (1994); D. Nehete, V. Shah, D.G. Kanhere, Phys. Rev. B **53**, 2126 (1996); V. Shah, D.G. Kanhere, J. Phys.: Cond. Matt. **8**, L253 (1996); V. Shah, D.G. Kanhere, C. Majumber, G.P. Das, *ibid.* **9**, 2165 (1997); A. Vichare, D.G. Kanhere, J. Phys.: Cond. Matt. **10**, 3309 (1998); A. Vichare, D.G. Kanhere, Eur. Phys. J. D **4**, 89 (1998); A. Dhavale, V. Shah, D.G. Kanhere, Phys. Rev. A **57**, 4522 (1998).
24. N. Govind, J.L. Mozos, H. Guo, Phys. Rev. B **51**, 7101 (1995); Y.A. Wang, N. Govind, E.A. Carter, *ibid.* **58**, 13465 (1998).
25. V. Bonacić-Koutecký, J. Jellinek, M. Wiechert, P. Fantucci, J. Chem. Phys. **107**, 6321 (1997); D. Reichardt, V. Bonacić-Koutecký, P. Fantucci, J. Jellinek, Chem. Phys. Lett. **279**, 129 (1997).
26. S. Kümmel, P.-G. Reinhard, M. Brack, Eur. Phys. J. D **9**, 149 (1999); S. Kümmel, M. Brack, P.-G. Reinhard, Phys. Rev. B **62**, 7602 (2000).
27. I.L. Garzón, K. Michaelian, M.R. Beltrán, A. Posada-Amarillas, P. Ordejón, E. Artacho, D. Sánchez-Portal, J.M. Soler, Phys. Rev. Lett. **81**, 1600 (1998).
28. J.M. Soler, M.R. Beltrán, K. Michaelian, I.L. Garzón, P. Ordejón, D. Sánchez-Portal, E. Artacho, Phys. Rev. B **61**, 5771 (2000).
29. J.P.K. Doye, D.J. Wales, J. Phys. B **29**, 4859 (1996).
30. *Theory of the inhomogeneous electron gas*, edited by S. Lundqvist, N.H. March (Plenum Press, New York, 1983).
31. W. Yang, Phys. Rev. A **34**, 4575 (1986).
32. J.P. Perdew, Phys. Lett. A **165**, 79 (1992).
33. J.P. Perdew, A. Zunger, Phys. Rev. B **23**, 5048 (1981).
34. D. Ceperley, B. Alder, Phys. Rev. Lett. **45**, 566 (1980).
35. C. Fiolhais, J.P. Perdew, S.Q. Armster, J.M. McLaren, H. Brajczewska, Phys. Rev. B **51**, 14001 (1995); *ibid.* **53**, 13193 (1996).
36. L. Verlet, Phys. Rev. **159**, 98 (1967); W.C. Swope, H.C. Andersen, J. Chem. Phys. **76**, 637 (1982).
37. M. Bockstedte, A. Kley, J. Neugebauer, M. Scheffler, Comp. Phys. Commun. **107**, 187 (1997).
38. S. Sugano, *Microcluster Physics* (Springer-Verlag, Berlin, 1991).
39. F. Ercolessi, W. Andreoni, E. Tosatti, Phys. Rev. Lett. **66**, 911 (1991).